Robustness of Interdependent Directed Higher-order Networks Against Cascading Failures

Dandan Zhao[a], Xianwen Ling[a], Hao Peng[a,b], Ming Zhong[a], Jianmin Han[a], Wei Wang[c]

[a]*College of Computer Science and Technology Zhejiang Normal University Jinhua 321004 Zhejiang China*
[b]*Shanghai Key Laboratory of Integrated Administration Technologies for Information Security, Shanghai, 200240, China*
[c]*School of Public Health, Chongqing Medical University, Chongqing, 400016, China*

Abstract

In the real world, directed networks are not just constructed as pairs of directed interactions, but also occur in groups of three or more nodes that form the higher-order structure of the network. From social networks to biological networks, there is growing evidence that real-world systems connect the functional relationships of multiple systems through interdependence. To understand the robustness of interdependent directed higher-order networks, we propose a new theoretical framework to model and analyze the robustness of such networks under random failures by percolation theory. We find that adding higher-order edges makes the network more vulnerable which quantifies and compares by two criteria: the size of the giant connected components and the percolation threshold. Increasing the hyperdegree distribution of heterogeneity or the hyperedge cardinality distribution of heterogeneity in interdependent directed higher-order networks will also make the network more vulnerable. Interestingly, the phase transition type changes from continuous to discontinuous with the increase of coupling strength, and partially interdependent directed higher-order networks exist hybrid phase transition. Moreover, by applying our theoretical analysis to real interdependent directed higher-order networks further validated our conclusion, it has implications for the design of flexible complex systems.

Keywords: Higher-order networks, Percolation, Phase transition

1. Introduction

In the real world, complex systems can be modeled as complex networks, where nodes represent individuals or components and edges represent interactions between them, such as biological

*Corresponding author
Email address: wwzqbx@hotmail.com (Wei Wang)

systems, social systems, and infrastructure [1, 2, 3, 4, 5]. However, directed pairwise interactions do not exist only between nodes, but also occur in groups of three or more nodes, which are considered directed higher-order structures in the network [6, 7, 8, 9]. For example, (Bio)chemical reactions are a typical example of higher-order directed processes, as, though some reactions can be reversible, there is often a privileged direction due to thermodynamics [10]. In addition, the ecology of microbial communities also have higher-order directional relationships, such as directional interactions between two species that affect another species [11, 12].

As a vital method to quantify the damage of a real system under random attacks [13, 14] or targeted attacks [15], the percolation theory can be utilized to investigate network connectivity and the robustness of directed networks [3, 16], such as the bond percolation [17], site percolation [18], and k-core percolation [19, 20]. For the bond (site) percolation, each edge (node) is occupied with probability p. With the increase of the occupation probability p, the network's giant strongly connected component (GSCC) gradually increases. When the GSCC changes from zero to nonzero, the occupation probability p_c is called the percolation threshold. These properties can be characterized by using percolation theory to analyze [21, 22].

Research on higher-order networks has aroused the interest of many scholars [23]. Higher-order networks have been considered in evolutionary dynamics [24], in the evolution of honesty [25], and in many dynamical processes, such as synchronization [26, 27] and all these phenomena are strongly dependent on robustness against cascading failures.

Understanding the robustness and resilience of the interdependent networks is crucial for designing and managing reliable and efficient systems. Such higher-order networks can capture the complexity and heterogeneity of real-world systems more accurately compared to traditional networks [28]. Peng *et al.* [29] constructed a theoretical model of a two-layer partial dependence network with simplicial complexes and introduce percolation theory to study the robustness of the network and find the density of the triangle and the dependent strength between the two networks affect the percolation behaviours of the network together. Bonamassa *et al.* [30] discovered an isomorphism between the ground state of random multispin models and interdependent percolation on randomly coupled networks. Because networks in the real world are not isolated, multi-layer networks need to be built to understand the robustness of interdependent directed higher-order networks [31, 32, 33, 34].

This article aims to study interdependent directed higher-order networks, which are networks where nodes are connected through directed hyperedges that capture higher-order interactions. These hyperedges can represent complex dependencies or interactions among nodes, such as group interactions [35, 36], information flow in social networks [37, 38], or regulatory interactions in biological networks [39, 40, 41]. The directed nature of the hyperedges introduces additional complexity and dynamics to the network, as the interactions among nodes may have directional dependencies. Adding higher-order directed edges enhances the robustness of the complex system and increasing the hyperdegree distribution of heterogeneity or the hyperedge cardinality distribu-

tion of heterogeneity in higher-order networks will make the network weakening the higher-order network's robustness [42]. In this paper, we explore the cascade failure process of interdependent networks on the basis of single-layer networks, and find different phenomena of percolation phase transition. Besides, breakdown of interdependent directed networks has been studied, and apply it to real-world international trade networks, and Liu *et al.* [43] found that the robustness of interdependent heterogeneous networks increases, whereas that of interdependent homogeneous networks with strong coupling strengths decreases with in-degree and out-degree correlations. Klosik et al. [44] designed a network of interdependent directed biomolecules which called the interdependent network of gene regulation and metabolism. The Network of gene regulation consists of 24,150 directed edges, and this network is interdependent on a protein network that can be represented by a higher-order network. By constructing a percolation model, they found that interdependent systems are sensitive to perturbations in gene regulation and protein levels, but robust to metabolic changes.

In this paper, we propose a new theoretical framework to model and analyze the robustness of interdependent directed higher-order networks using generating functions and percolation theory. We study the robustness of interdependent directed higher-order networks by quantifying two criteria: the size of the giant connected components(GIN, GOUT and GSCC) and the percolation threshold. We generate fully dependent and partially dependent directed higher-order networks by giving the hyperdegree k and the hyperedge cardinality m. The size of the giant connected components of each layer and the percolation threshold are calculated when the cascade failure reaches steady state and verified by numerical simulation. In summary, the main contributions of this paper are as follows.

- Proposing an interdependent directed higher-order networks theoretical framework to study the robustness of higher-order networks. Mathematical formulas deduce the percolation threshold and the size of different GCCs. The results of simulations and theoretical simulations correspond to the artificial network we constructed.

- The effects of hyperdegree and hyperedge cardinality distribution heterogeneity on interdependent directed higher-order networks are revealed. With the increase of network hyperdegree and hyperedge cardinality, the heterogeneity of hyperdegree distribution increases and the percolation threshold decreases. The cascade failure process of interdependent directed higher-order networks is analyzed. In addition, the phase transition type changes from continuous phase transition to hybrid phase transition and then to discontinuous phase transition with the increase of coupling strength.

- Our theory is validated on both artificial and real-world networks. We built social conference networks and biological neural networks, and combined real and artificial networks to simulate the percolation process of interdependent directed higher-order networks in the real world.

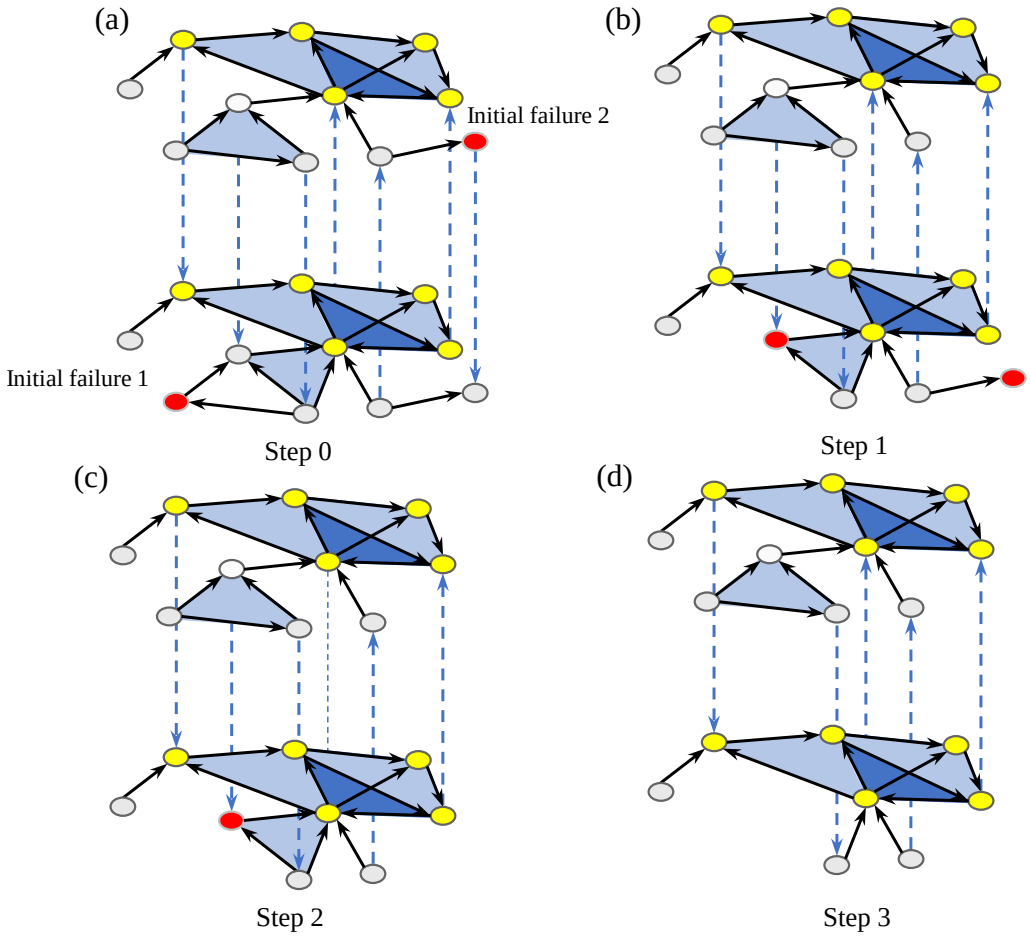

Figure 1: **Schematic representation of a cascading failure process on interdependent directed higher-order networks.** Panels **(a)-(d)**: Both network A and network B have 11 nodes, where $q_A = 3/11$ node depends on nodes in network B and $q_B = 4/11$ node depends on nodes in network A. In the initial cascading failure, the nodes in red represent the nodes removed from the network, from the initial step 0 to step 3, showing the process of partially interdependent cascading failures.

The work is organized as follows. In Section 2, we introduce a interdependent directed higher-order network model. In Section 3, we propose a framework for analyzing the robustness of interdependent directed higher-order networks and conduct a theoretical analysis. In Section 4, we present our process analysis of percolation and cascade failure, and the calculation of percolation threshold, followed by discussions in Section 5. Finally, we conclude the paper in Section 6 with a summary of our findings and directions for future research.

2. MODEL

Consider the interdependent directed higher-order networks A and network B in a system with the same number of network nodes. q_A represents the probability that network A is randomly connected to network B; q_B represents the probability that network B is randomly connected to network A. The interdependence between the two layers is defined by the links between the layers, through which full and partial dependencies are discussed. As in our previous work, we construct a higher-order directed network with a specific hyperdegree size k and hyperedge cardinality m.

After constructing the two-layer interdependent directed higher-order network, we set the initial removal probability of the network as p, that is, the initial retention probability of the network as $1-p$. With the failure of the nodes in network A, the nodes in network B are affected, and the cascading failures continue to iterate, and the number of network functional nodes continues to decrease. By converting the network into a factor graph, when the size of network A and network B is equal, the process of cascade failure ends, and the process reaches a steady state. Then we calculate the GCCs of the network, to study the robustness of the interdependent directed higher-order network. The strongly connected component in a directed network, where a vertex in GSCC can reach any other vertex in GSCC. The Giant In-component (GIN) and Giant Out-component (GOUT) is the nodes of GSCC plus the nodes leading to/from GSCC. For convenience, we use S to represent GSCC and S_i/S_o to represent GIN/GOUT The model is illustrated in Fig.(1).

3. THEORETICAL ANALYSIS

Before introducing higher-order directed networks, we need to know about hyperlink. Various orders of interactions, such as 1-hyperlink, 2-hyperlink, etc. The 2-hyperlink is an interaction among three nodes on hypergraphs. Our model represents directionality in the network by transforming the generated higher-order network into a directed factor graph.

Without losing generality, we define a directed higher-order network through mathematical language. In Alain Bretto's higher-order networks review, a directed higher-order network is defined as an ordered pair: $\vec{H} = (V; \vec{E} = (\{\overrightarrow{e_i} : i \in I)$, where V is a finite set of vertices and $\vec{E}$ is a set of hyperedge with finite index set I . Each hyperedge $\overrightarrow{e_i}$ is an ordered pair. Similar to the definition of a higher-order network given in Section 2.2, in a directed higher-order network, hyperedges represent the directed interaction of two vertices with directions. According to the

definition of the directed higher-order network $G_{DH}(V, U, E)$, which is essentially a bipartite graph, after all, V is the set of nodes, U represents a set of factor nodes, E of the edges between the nodes and the factor nodes, and each interaction connects a node one-way to a factor node. The factor graph is related to the directed higher-order network by simply mapping. In the directed higher-order network, we introduce the concepts of k_i and k_o to represent the size of the in- and out-degree of the higher-order network, referred to as the hyperdegree, which means the number of nodes connected to factor nodes. The number of factor nodes connected to nodes is represented by m_i and m_o, referred to as hyperedge cardinality.

The following is our theoretical derivation from the generating function. The definition of the generating function of the in- and out-hyperdegrees distribution of the initial network node is as follows,

$$G_0^A(x,y) = \sum_{k_i k_o} P\left(k_i, k_o\right) x^{k_i} y^{k_o}, \tag{1}$$

$$G_0^B(x,y) = \sum_{k_i k_o} P\left(k_i, k_o\right) x^{k_i} y^{k_o}, \tag{2}$$

where $P(k_i, k_o)$ is the joint degree distribution of a directed higher-order network, x and y denote any variable. Since the sum of the in- and out-hyperdegrees is zero, the $P(k_i, k_o)$ must satisfy the constraint

$$\sum_{k_i k_o} P(k_i, k_o)(k_i - k_o) = 0, \tag{3}$$

For the symmetric case with coupling strengths $q_A = q_B = q$, nonremoved nodes after initial failure $p_1 = p_2 = p$, and degree distributions $P_A\left(k_{\mathrm{i}}, k_{\mathrm{o}}\right) = P_B\left(k_{\mathrm{i}}, k_{\mathrm{o}}\right) = P\left(k_{\mathrm{i}}, k_{\mathrm{o}}\right)$. With G_0, we can define the generating functions G_0^i denotes the number of outward edges that leave a randomly chosen vertex the number of vertices leaving by following a randomly chosen edge, and G_1^i denotes the number leaving the vertex reached by following a randomly chosen edge [45],

$$G_1^A(x,1) = \frac{\partial_y G^A(x,y)\big|_{y=1}}{\partial_y G^A(1,1)}, \tag{4}$$

$$G_1^A(1,y) = \frac{\partial_x G^A(x,y)\big|_{x=1}}{\partial_x G^A(1,1)}. \tag{5}$$

Similarly, the generating functions of the branching process of network B,

$$G_1^B(x,1) = \frac{\partial_y G^B(x,y)\big|_{y=1}}{\partial_y G^B(1,1)}, \tag{6}$$

$$G_1^B(1,y) = \frac{\partial_x G^B(x,y)\big|_{x=1}}{\partial_x G^B(1,1)}. \tag{7}$$

We define the generating functions G_0^o and G_1^o for the number arriving at such a vertex,

$$G_0^o(x) = G_0(x,1), \tag{8}$$

$$G_1^o(x) = \frac{1}{k_o}\frac{\partial G_0(x,y)}{\partial y}\bigg|_{y=1}. \tag{9}$$

Average hyperdegree of a directed higher-order network,

$$\langle k\rangle = \sum_{k_i} P(k_i,k_o)k_i = \sum_{k_o} P(k_i,k_o)k_o. \tag{10}$$

Based on the definition of hyperedges, the generating function definition of the cardinality distribution of the in- and out-hyperedges of the initial network node is as follows:

$$\hat{G}_0^A(x,y) = \sum_{m_i m_o} \hat{P}\left(m_i,m_o\right) x^{m_i} y^{m_o}, \tag{11}$$

$$\hat{G}_0^B(x,y) = \sum_{m_i m_o} \hat{P}\left(m_i,m_o\right) x^{m_i} y^{m_o}, \tag{12}$$

where $\hat{P}(m_i,m_o)$ is the joint degree distribution of a directed higher-order network, x and y denote any variable. Since the sum of the in- and out-hyperedge cardinality is zero, the $\hat{P}(m_i,m_o)$ must satisfy the constraint

With $\hat{G}_0$, we can define the generating functions $\widehat{G}_0^i$ for the number of outward points leaving a randomly chosen factor of the node, and $\widehat{G}_1^i$ for the number of points leaving a factor of the node by following a randomly chosen edge,

$$\hat{G}_0^i(y) = \hat{G}_0(1,y), \tag{13}$$

$$\hat{G}_1^i(y) = \frac{1}{m_i}\frac{\partial \hat{G}_0(x,y)}{\partial x}\bigg|_{x=1}. \tag{14}$$

In the same way, we can define the number of generating functions $\widehat{G}_0^o$ and $\widehat{G}_1^o$ for the number arriving at such a vertex,

$$\hat{G}_0^o(x) = \hat{G}_0(x,1), \tag{15}$$

$$\hat{G}_1^o(x) = \frac{1}{m_o}\frac{\partial \hat{G}_0(x,y)}{\partial y}\bigg|_{y=1}. \tag{16}$$

The average cardinality of the directed higher-order network,

$$\langle m\rangle = \sum_{m_i} \hat{P}\left(\ m_i,\ m_o\right) m_i = \sum_{m_o} \hat{P}\left(\ m_i,\ m_o\right) m_o. \tag{17}$$

With the idea of the factor graph, given the hyperdegree size k_i and k_o, and the hyperedge cardinality m_i and m_o, we can get four parameters to quantify the network. To simplify the network, we set $k = k_i = k_o$ and $m = m_i = m_o$. Given that the initial number of nodes in the network is N, we calculate the number of factor nodes in the network due to the relationship between k and m in the factor graph:$N_{factor} = N * k/m$. With the given parameters above, we can construct the directed random higher-order network conforming to the hyperdegree size k and the hyperedge cardinality m.

As shown in Fig.1(a), we will have a model to generate the higher-order network divided into two steps. In the first step, a specific degree sequence was generated for the random network through the degree distribution function. The second step: is through the method of random connections, combined with the introduction of the model previously defined by the concept of a random triangle, to generate the different directed random triangles and generate the directed higher-order network. [46].

In our directed higher-order network model, the network structure is random and sparse, so for a large enough network, it can be considered as a tree. That is, there is no circle in the network. The percolation problem of a directed higher-order network can be solved accurately by generating functions. To represent the initial degree distribution of a higher-order network, we define the hyperdegree distribution $P(k)$ and the hyperedge cardinality distribution $\hat{P}(m)$ correspond to the degree distributions of the nodes and factor nodes in the factor graph, respectively [47].

As a random higher-order network map's component graph is a local tree, we take into account its corresponding factor graphs to depict percolation on directed higher-order networks. We can use a self-consistent equation to represent the probability of reaching a factor node belonging to the GCC from a node along with the edge,

$$\hat{S} = \sum_{m} \frac{m}{\langle m \rangle} \hat{P}(m) \left[1 - (1 - S)^{m-1}\right]. \tag{18}$$

In Eq.(18), $m - 1$ means that the factor node removes the edge from which it originates, $(1 - S)^{m-1}$ represents the probability that a factor node cannot reach a node from the GCC, take the sum and average over all the probabilities, we can get the $\hat{S}$. In the same way, $(1 - S)^{k-1}$ represents the probability that a normal node cannot reach a factor node from the GCC, S is the probability that a node from a node belongs to a GCC,

$$S = p \sum_{k} \frac{k}{\langle k \rangle} P(k) \left[1 - (1 - \hat{S})^{k-1}\right]. \tag{19}$$

The order parameters of the percolation process, which are given by the probability R of finding

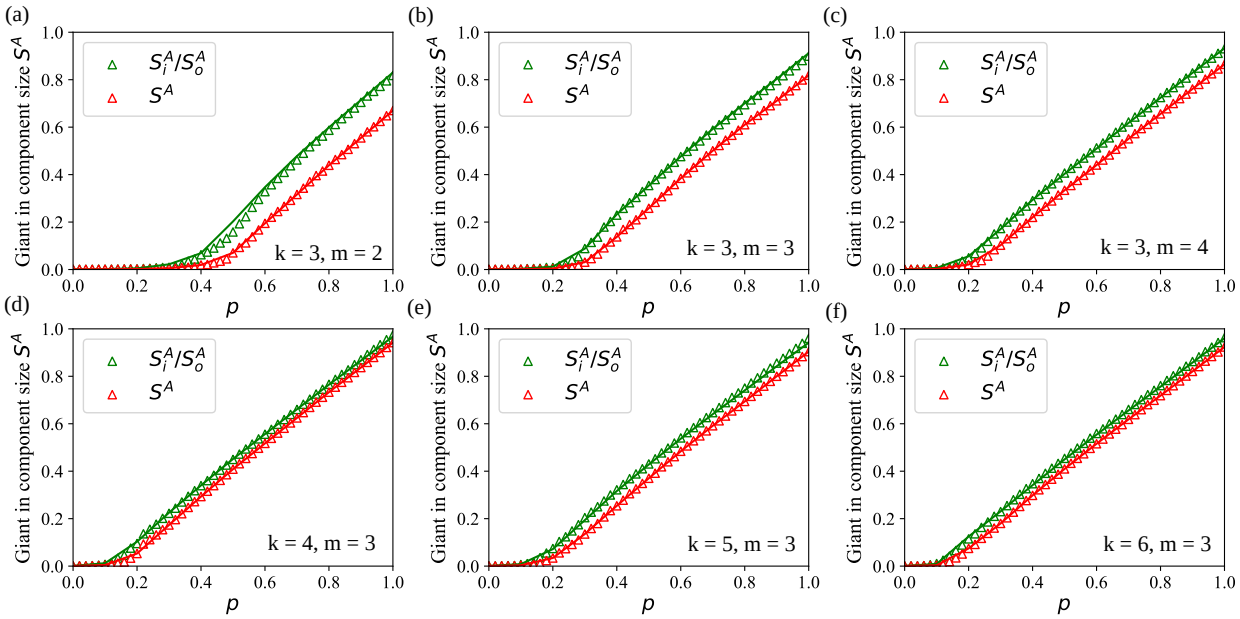

Figure 2: **Percolation on the fully interdependent directed higher-order networks.** Experiment under different conditions: Panel **(a)-(f)** $k \in \{2, 3, 4\}$, $m \in \{2, 3, 4\}$. With the increase of node removal probability $1 - p$, the process of network disintegration is expressed by the size change of GCCs and the change of percolation threshold in the network. The percolation simulation of the directed higher-order network is consistent with the theory.

a node in the GCC and the probability $\hat{R}$ of finding a hyperedge in the GCC,

$$R = 1 - \sum_{k} P(k)(1-\hat{S})^{k}, \tag{20}$$

$$\hat{R} = 1 - \sum_{m} \hat{P}(m)(1-S)^{m}. \tag{21}$$

Eqs(17)-(21) can be used to investigate the fundamental aspects of percolation and determine how robust higher-order networks are. In the directed higher-order networks, we consider the probability of finding a node in a GCC as the order parameter R to characterize the percolation problem. Through the definition of the giant in-component and the giant out-component, we give the formula of R_i and R_o ,

$$R_i = p\left\{1 - \sum_{io} P_i(i,o)(1-\hat{s})^{i}\right\}, \tag{22}$$

$$R_o = p\left\{1 - \sum_{io} P_o(i,o)(1-\hat{s})^{o}\right\}. \tag{23}$$

Using the generating function $G_0(x,y)$, the above equation can be simplified as

$$R_i = p\left\{1 - G_0\left(1-\hat{s}_i, 1\right)\right\}, \tag{24}$$

$$R_o = p\left\{1 - G_0\left(1, 1-\hat{s}_o\right)\right\}. \tag{25}$$

Eq.(17) and Eq.(23) give the relationship between the directed higher-order network R_i and S_i, R_o and S_o, but based on this formula, S or R cannot be solved. Therefore, we use Eq.(16) in Peng et al. [15], to derive the following formula,

$$\hat{S} = 1 - \hat{H}_1(1-S), \tag{26}$$

$$S = p\left(1 - H_1(1-\hat{S})\right). \tag{27}$$

The generating function in the undirected random higher-order network represented by H in the formula.

Since directed higher-order networks can also be mapped to factor graphs, we give formulas for S and $\hat{S}$,

$$\hat{S}_i = \sum_{m_i m_o} \frac{m}{\langle m \rangle} P(m_i, m_o)\left[1 - (1-\hat{S}_i)^{m-1}\right], \tag{28}$$

$$S_i = p\sum_{k_i k_o} \frac{k}{\langle k \rangle} P(k_i, k_o)\left[1 - \left(1-\hat{S}_i\right)^{k-1}\right]. \tag{29}$$

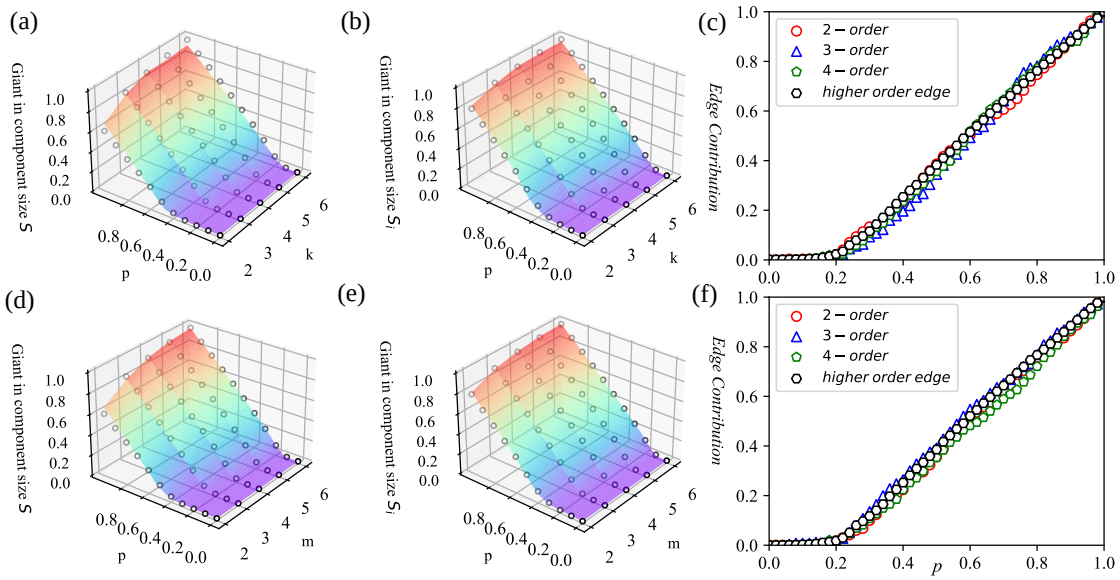

Figure 3: **The three-dimensional diagram of the percolation of the fully interdependent directed higher-order networks and the contribution of higher-order edges and lower-order edges in the directed random higher-order network.** The three-dimensional graph **(a),(b),(d),(e)** corresponds to the percolation of the directed random higher-order network. The coordinates of the X-axis represent the hyperedge cardinality m of the network and the size of the hyperdegree k. The Y-axis represents the probability of retaining nodes in the network p, and the Z-axis represents the probability of retaining nodes in the network S_i and S. Since S_i and S_o are equal in size, only S_i is shown here for brevity. Panel **(c),(f)**: The circle, triangle, pentagon, and hexagon in the graph respectively represent the size of hyperedges of different orders. The vertical axis represents the proportion of the number of edges of this order based on the size of the initial network.

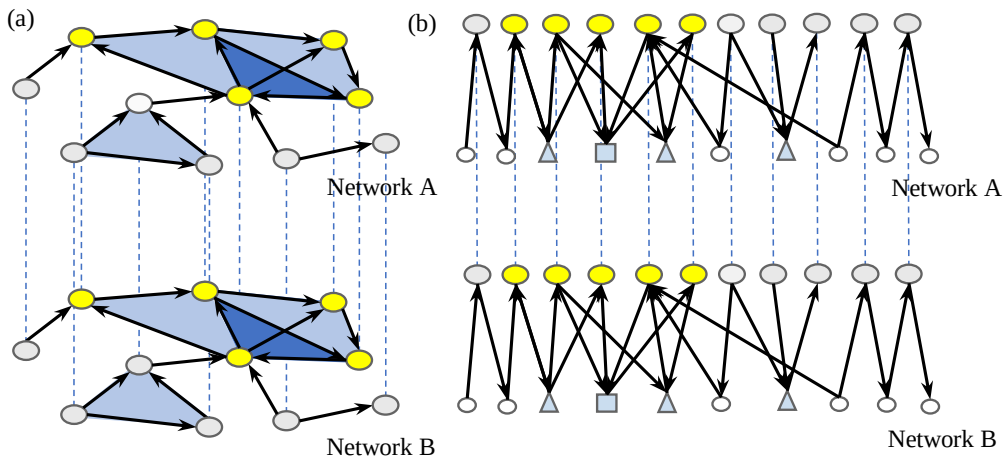

Figure 4: **Schematic on a higher-order directed interdependent network and transform into a factor graph.** The interdependencies between network A and network B are represented by blue dashed lines. Panel **(a)** Higher-order network A and network B are completely interdependent through coupling. The elliptic nodes in the figure represent the nodes in the higher-order network, and the blue graphs of different shapes represent the hyperedges of different orders. Yellow nodes represent the giant strongly connected component(GSCC) of the network. Panel **(b)** Convert the higher-order directed network in Fig1.(a) into a factor graph, where the upper layer represents the nodes in the network, and the white and blue nodes in the lower layer represent the hyperedges of different sizes.

Similarly, we derive the formula for S_o and $\hat{S}_o$,

$$\hat{S}_o = \sum_{m_i m_o} \frac{m}{\langle m \rangle} P(m_i, m_o) \left[1 - (1 - \hat{S}_i)^{m-1}\right], \tag{30}$$

$$S_o = p \sum_{k_i k_o} \frac{k}{\langle k \rangle} P(k_i, k_o) \left[1 - \left(1 - \hat{S}_i\right)^{k-1}\right]. \tag{31}$$

To simplify the above formula,

$$\hat{S}_d = 1 - \left(1 - \hat{G}_1(S_d, 1)\right), \tag{32}$$

$$S_d = 1 - p(1 - G_1(1, \hat{S}_d)). \tag{33}$$

We calculate the size of the GSCC from the original generating function,

$$S = \sum_{k_\mathrm{i}, k_\mathrm{o}} P\left(k_\mathrm{i}, k_\mathrm{o}\right) \left(1 - x_c^{k_\mathrm{i}}\right) \left(1 - y_c^{k_\mathrm{o}}\right) = 1 - G\left(x_c, 1\right) - G\left(1, y_c\right) + G\left(x_c, y_c\right). \tag{34}$$

Then convert the above formula,

$$g_{_A}(p) = 1 - G_0^A \left(\hat{S}_{_d}, 1\right), \tag{35}$$

$$g_{_B}(p) = 1 - G_0^B \left(1, \hat{S}_{_d}\right). \tag{36}$$

The size of $g_{_A}(p)$ and $g_{_B}(p)$ can be calculated from this formula.

In Buldyrev's two-layer network, we also randomly delete part of the nodes and part of the B nodes. The network is segmented into each strongly connected component, where each pair of nodes can reach each other through a directed path. Only the GSCC is considered a potential functional node. Therefore, after the initial node is removed, the size of the function A node and function B node (GSCC), respectively, $\psi_1 = p_1 g_A(p_1)$ and $\phi_1 = p_2 g_B(p_2)$. And the formula $g_{_A}(p)$ and $g_{_B}(p)$ calculates the size of GSCC in network isolation and isolated network B respectively, x and y denote any variable.

Here we define $f_A(p)$ and $f_B(p)$,

$$f_A(p) = G_0^A \left(\hat{S}_d, 1\right), \tag{37}$$

$$f_B(p) = G_0^B \left(1, \hat{S}_d\right). \tag{38}$$

At the end of the cascade failure, we arrive at two symmetric equations of a system with two unknowns,

$$x = p g_a(y), \tag{39}$$

$$y = p g_b(x). \tag{40}$$

This system of equations has a trivial solution $x = 0, y = 0$ corresponding to a giant component of size $p = 0$. If p is large enough there exists a different solution, given the non-zero size of the common giant components. We can easily exclude from these equations and get an equation y,

$$x = pg_a(pg_b(x)). \tag{41}$$

We can use this formula to figure out the magnitude of x. On account of $R = x * g_b(x)$, derive the sizes of R_i and R_o.

$$R_{\mathrm{i}}^A = R_o^A = x * \left[1 - G_0^A\left(1, \hat{S}_d\right)\right], \tag{42}$$

$$R_{\mathrm{i}}^B = R_o^B = x * \left[1 - G_0^B\left(1, \hat{S}_d\right)\right]. \tag{43}$$

Since in Eq.(32) before, we calculate the $\hat{S}_d$, from this self-consistent equation the magnitude of $\hat{S}_d$ can be derived, and thus the magnitude of R_i and R_o can be calculated.

4. Experimental results and analysis

We use artificially constructed networks to study the robustness of fully interdependent and partially interdependent directed higher-order networks. We measure the robustness of the network by calculating the GIN/GOUT, GSCC and the percolation threshold.

4.1. Fully dependent higher-order directed network

We perform Monte-Carlo simulations of the generated networks by constructing homogeneous directed higher-order networks. Different percolation experimental results are obtained by changing the network with different hyperdegree k and hyperedge cardinality m. It can be seen that the percolation threshold tends to decrease as the product of hyperdegree k and hyperedge cardinality m increases. The network's three GCCs undergo phase transitions simultaneously, and the sizes of the GIN and the GOUT are larger than the GSCC after the phase transition point.

The critical points of S_i and S_o of the directed higher-order network are the same as those of the tree random directed network and have nothing to do with the degree distribution and the correlation between the in-and out-degree. The GIN and the GOUT appear together with the GSCC, and it is impossible to emerge as one of them alone. Therefore, the critical points of the GIN and the GOUT of the homogeneous directed higher-order networks are the same, and the critical points of the GSCC are the same, which is confirmed by the simulation results.

To simplify the model, we set the average hyperdegree is $\langle k \rangle = \langle k_i \rangle = \langle k_o \rangle$ and the average hyperedge cardinality $\langle m \rangle = \langle m_i \rangle = \langle m_o \rangle$.

Insights that emphasize distinctive groupings and unique functional contributions of network nodes have received priority in the majority of network science discoveries. Importantly, the

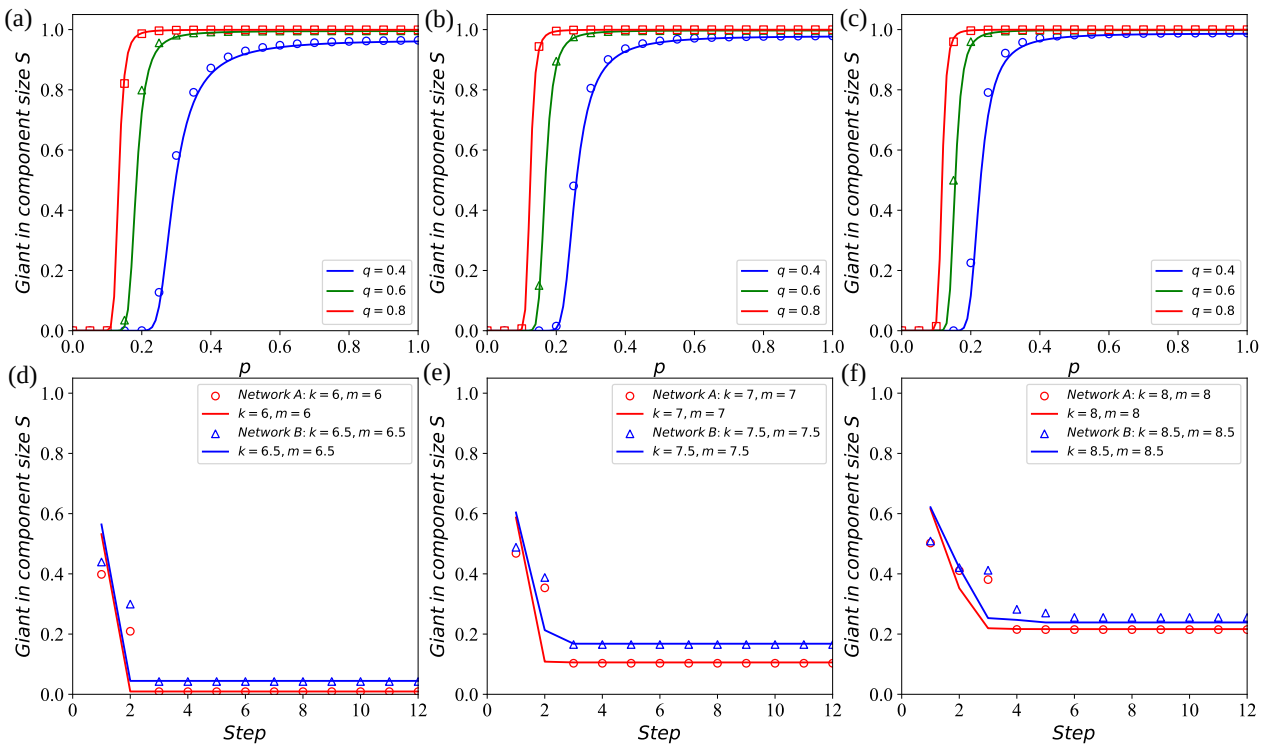

Figure 5: **Percolation on the partially interdependent directed higher-order networks and the dynamic process of cascading failure.** Panel **(a)-(c)**: Change $q = \{0.4, 0.6, 0.8\}$, the percolation process of partially interdependent directed higher-order networks under different p values. Panel **(d)-(f)**: The red solid line is the analysis result of GSCC size of network A at each stage of the cascade fault, and the blue line is the analysis result of GSCC size of network B, which is in good agreement with the simulation result expressed by symbol ($N = 10^4$). In the simulation, we set the $\langle k_A \rangle = \{6, 7, 8\}$,$\langle k_B \rangle = \{6.5, 7.5, 8.5\}$, $q_A = 0.4$, $q_B = 0.5$, $p_1 = 0.5$, $p_2 = 0.6$.

network of their interrelationships, generated by network edges, determines and expresses these functional contributions [48]. In order to better understand the importance of different hyperedges in a directed higher-order network, based on our directed higher-order network model, we study the contribution of each edge under relative initial GSCC. Without edges, a directed higher-order network would be a set of nodes without interaction.

In the experiment shown in Fig. 3, we counted the number of hyperedges of different orders in the strongly connected components, and expressed it by the contribution of edges, that is, the proportion of the number of hyperedges in the initial number of hyperedges in the percolation process. It can be seen from the experiment that the curve of edge contribution tends to be consistent with the curve of percolation in experiment part A. In the real network, we can use the experimental results to control the slump of the number of hyperedges.

Based on our simulation results, it can be seen that Panel (c) and (f) in Fig. 3 represent the contribution of hyperedges in the directed higher-order network. In the simulation results, we find that the number of hyperedges is significantly larger than that of low-order edges and that higher-order interactions play a more vital part in the percolation of higher-order networks. In addition, we also calculate the number of hyperedges of different orders in GSCC, including 2-order edges, 3-order edges, and 4-order edges. When the node retention probability p is decreasing, and the removal probability $1-p$ increases, the size of the network decreases gradually, and the number of hyperedges decreases continuously.

4.2. Partially dependent higher-order directed network

We present the solution for the final GSCC size step by step according to the cascading process, as shown in Fig. 5.

Different from the fully dependent higher-order directed network, the connection of the partially dependent higher-order directed network is unidirectional and random. Here, we define A uniform q_A to represent the probability that network A connects to network B. q_B represents the probability that network B is connected to network A. In the initial partially interdependent network, we study the percolation through the retention probability of $1-p$, and explore the robustness of the higher-order directed network.

With the removal of nodes in network A, due to the existence of interdependent edges between nodes, the interdependent edges of broken nodes connected to network A, and the nodes in network B are also affected, and the functional nodes fail. The feedback obtained in this process is the first step of network cascade failure. Such steps are iterated continuously, and when network A and network B reach steady state, we can calculate the network's GSCC,

$$S^A = \frac{\left(1-z_{\mathrm{i}}^A\right)\left(1-G_0^A\left(z_{\mathrm{i}}^A, z_{\mathrm{o}}^A\right)\right)}{1-G_1^A\left(z_{\mathrm{i}}^A, 1\right)}, \tag{44}$$

$$S^B = \frac{\left(1-z_{\mathrm{i}}^B\right)\left(1-G_0^B\left(z_{\mathrm{i}}^B, z_{\mathrm{o}}^B\right)\right)}{1-G_1^B\left(z_{\mathrm{i}}^B, 1\right)}, \tag{45}$$

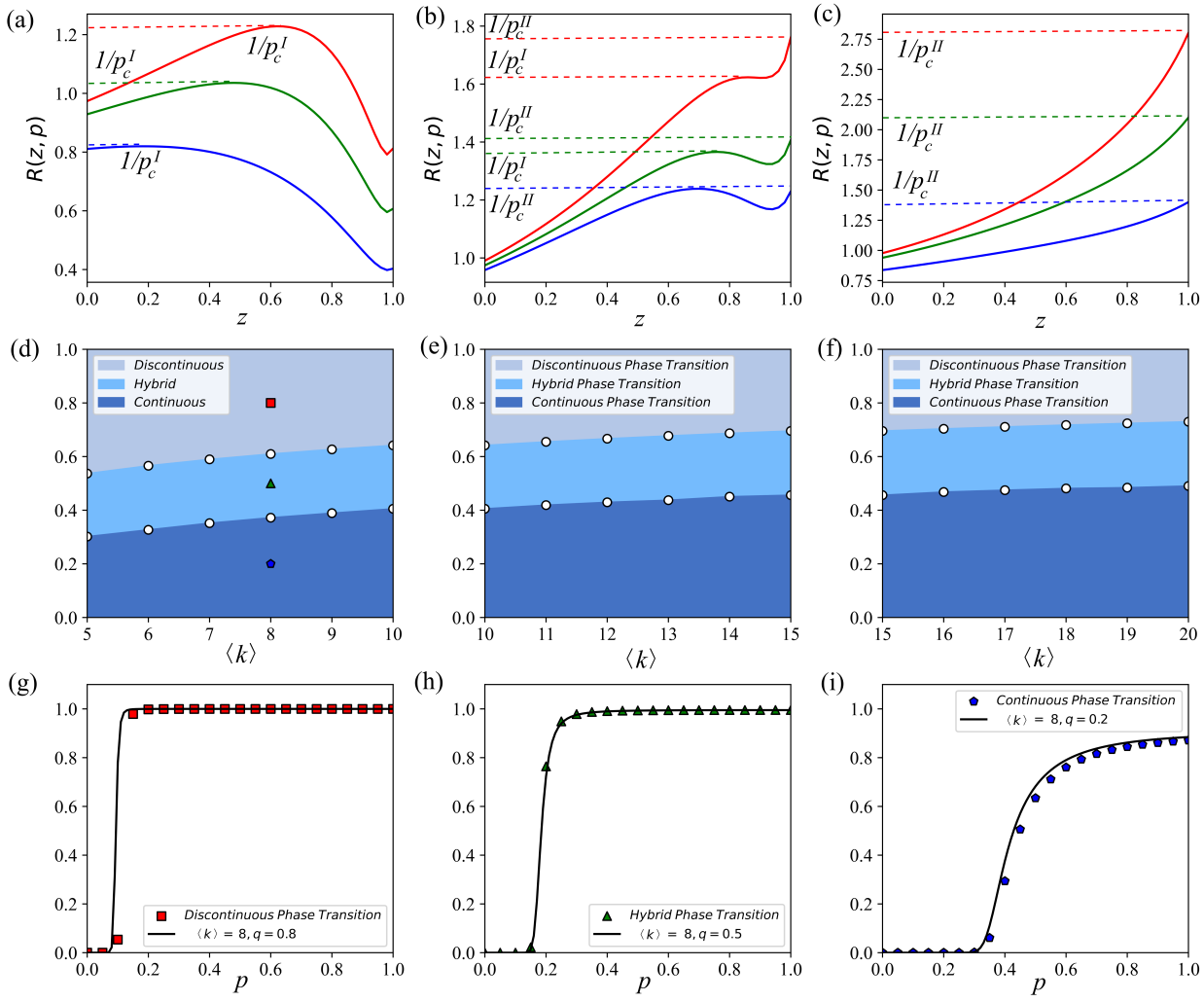

Figure 6: **Percolation thresholds of interdependent directed higher-order networks and phase diagrams.** Using the function R analysis calculation to analyze the percolation behavior, we set $k = 8$, $m = 4$. Panel **(a)**: We set the connection probability q between network A and network B to 0.8, we can see the discontinuous phase transition, function R has a maximum value, At this time, the corresponding threshold $P_c^I = 0.877$. Panel **(b)**: When the connection probability q between network A and network B is 0.65, it can be found that the function has A maximum value and a maximum value, which are $P_c^I = 0.735$ and $P_c^{II} = 0.709$ respectively. Panel **(c)**: When the connection probability q between network A and network B is 0.3, it can be found that the function increases monotonically, in which case $z = 1$ has a maximum $P_c^{II} = 0.3125$. Panel **(e)-(f)**: In the case of different k values, whether the interdependent directed higher-order network will undergo discontinuous phase transition or continuous phase transition. Panel **(g)-(i)**: The squares, triangles and pentagons in Panel **(e)** correspond to Panel **(g)-(i)**, showing discontinuous phase transition, hybrid phase transition and continuous phase transition in the process of percolation phase transition respectively.

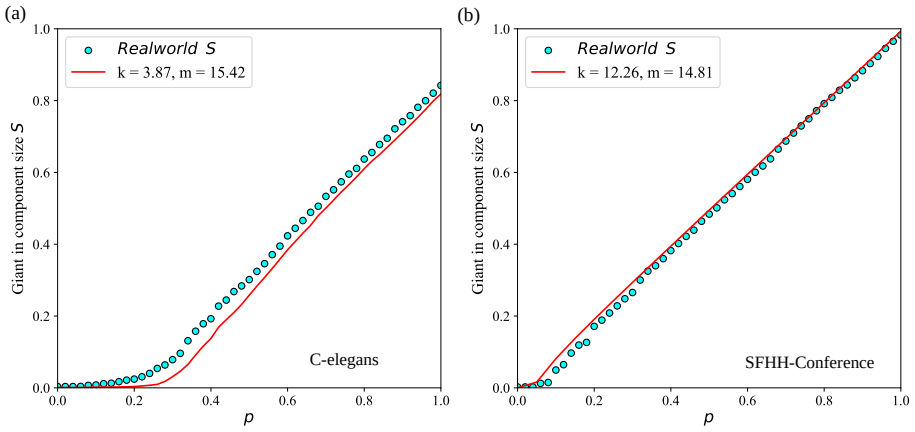

Figure 7: **Percolation on the real-world data sets: biological neural networks and the social networks.** Panel **(a)** are factor graphs transformed from real networks, representing friendship networks and neuron networks, respectively. Blue lines in the figure represent edges in factor graphs, while triangles, squares and pentagons represent hyperedges or factor nodes in factor graphs. Panel **(b)** in the figure is the percolation results and corresponding theoretical solutions. The corresponding theoretical parameters are shown in Table 1, and the ordinate coordinates correspond to the GIN, GOUT and GSCC sizes of the network, respectively.

where z_i^A, z_i^B,z_o^A and z_o^B are arbitrary complex variables. If we convert the above formula, we get

$$\frac{1-z_{\mathrm{i}}^A}{1-G_1^A\left(z_{\mathrm{i}}^A,1\right)}=p_1\left(1-q_A\left(1-\left(1-G^B\left(z_{\mathrm{i}}^B,z_{\mathrm{o}}^B\right)\right)p_2\right)\right), \tag{46}$$

$$\frac{1-z_{\mathrm{i}}^B}{1-G_1^B\left(z_{\mathrm{i}}^B,1\right)}=p_2\left(1-q_B\left(1-\left(1-G^A\left(z_{\mathrm{i}}^A,z_{\mathrm{o}}^A\right)\right)p_1\right)\right). \tag{47}$$

We set $q_A=q_B=q$ and $p_1=p_2=p$ into the above formula, we can calculate the network's GSCC. When the joint degree distribution of network A and B is the same, N tends to infinity, $S^A=S^{A'}$, $S^B=S^{B'}$. Through the above derivation,

$$\begin{aligned} x_A &= G_1^A\left(p_1x_A+1-p_1,1\right), &(48)\\ y_A &= G_1^A\left(1,p_1y_A+1-p_1\right), &(49)\\ x_B &= G_1^B\left(p_2x_B+1-p_2,1\right), &(50)\\ y_B &= G_1^B\left(1,p_2y_B+1-p_2\right). &(51)\end{aligned}$$

The GSCC belonging to network A after removing $1-p_1$ nodes,

$$\begin{aligned} S_A\left(p_1\right) &= 1-G_0^A\left(p_1x_A+1-p_1,1\right), &(52)\\ S_B\left(p_1\right) &= 1-G_0^B\left(p_1x_B+1-p_1,1\right). &(53)\end{aligned}$$

At the end of the cascade failure, we calculate the size of the final GSCC,

$$S^{A\prime} = p_1\left(1-q_A\left(1-p_B\left(S^{B\prime}\right)p_2\right)\right), \tag{54}$$
$$S^{B\prime} = p_2\left(1-q_B\left(1-p_A\left(S^{A\prime}\right)p_1\right)\right). \tag{55}$$

Then we discuss the critical threshold of percolation under different coupling strength (0-1), and find the interesting phenomenon of dependent directed higher-order network.
When the coupling strength is set greater than the continuous phase transition point q_{c2}, when there is a continuous phase transition, when z tends to 1, R_{i}^A is a monotone increasing function. R_{i}^A is monotone increasing function of z= 1, R_{i}^A is the largest. With this revised generating function, the percolation threshold can be written

$$P_c^{II} = \frac{1}{\lim_{z\to 1} R_i^A(z_c,q)} = \frac{1}{G_1^{A\prime}(1,1)(1-q)}. \tag{56}$$

The result of both percolation thresholds is the inverse of the corresponding p_c^{II}. When the degree and hyperedge cardinality of interdependent directed higher-order networks conform to a Poisson distribution, we can denote the average degree as

$$\langle k_{aver}\rangle = \langle k\rangle\langle m\rangle. \tag{57}$$

For such interdependent directed higher-order networks conforming to k and m, the percolation threshold can be reduced to $p_c^{II} = 2/(\langle k_{aver}\rangle(1-q))$. When the coupling strength is set less than the discontinuous phase change point q_{c1},

$$P_c^{I} = \frac{1}{R_i^A(z_c,q)}, \tag{58}$$

where $R_i^A(z_c,q)$ as a function of z has a peak at z_c which is the smaller root of $F_i^A(z_c,q)=0$, and $F_i^A(z,q)$ is the first derivative of $R_i^A(z_c,q)$.

The solutions of the critical coupling strengths q_{c2} and q_{c1} by numerical simulations have been proposed by Zhou et al. [49].

5. APPLICATION TO REAL NETWORKS

To confirm the accuracy of the results obtained from the manual dataset, we construct real interdependent directed higher-order networks in different scenarios. Directed networks are widely used in higher-order real networks, including biological networks and social networks. Here are two real network datasets applied in our experiment:

Table 1: The actual parameters in the real network, including the number of nodes N, the number of edges E, the average size of hyperdegree $\langle k \rangle$ and hyperedge cardinality $\langle m \rangle$, the maximum in- and out-hyperdegree $\boldsymbol{k}_{in}^{\max}$ $\boldsymbol{k}_{out}^{\max}$ and the maximum hyperedge cardinality $m_{\max}$, $\{E1, E2, E3, E4, E5\}$ represents hyperedges of different sizes of the initial network.

Dataset	N	E	$\langle k \rangle$	$\langle m \rangle$	$\boldsymbol{k}_{in}^{\max}$	$\boldsymbol{k}_{out}^{\max}$	$m_{\max}$	$E1$	$E2$	$E3$	$E4$	$E5$
C-elegans	279	2194	3.87	15.43	48	53	97	2010	48	44	75	73
SFHH-Conference	2446	70261	12.26	14.81	2120	2217	2446	60378	7503	1776	429	175

Neuronal networks (C-elegans) [50]: This dataset calculates the topological properties of neuronal networks, such as degree distributions, synaptic multiplicity, and small-world properties. Nodes are different neurons. Using linear systems theory, the authors investigated how brain activity spreads in response to sensory or artificial stimuli and discovered a number of patterns of activity that might work as the behavioral substrates mentioned previously. Analyzed is the relationship between the chemical synaptic network and the gap junction.

Social networks (SFHH-Conference) [51]: This data set describes the face-to-face interactions of 405 participants to the 2009 SFHH conference in Nice, France (June 4-5, 2009). It was first described in the publications Dynamics of Person-to-Person Interactions from Distributed RFID Sensor Networks and Simulation of an SEIR Infectious Disease Model on the Dynamic Contact Network of Conference Attendees.

To enhance the efficiency of the experiment, Table 1's listing of seven parameters for the artificial network experiment.

In each real-world dataset, we build a real network by the method of the previous work Ref. 38. By measuring the number of nodes in the real network, hyperdegree k and hyperedge cardinality m, we first construct the artificial higher-order network. Then we connect the real directed higher-order networks through the completely dependent edge, to generate the dependent directed higher-order network we need. The results represent cascade failures caused by structural failures and do not represent failures caused by real dynamics, such as those caused by overloads in PG network systems [52].

With the decrease of the probability of retaining nodes in the factor graph, we find that the size of the GSCC in the real directed higher-order network gradually decreases, and a phase transition occurs at the percolation threshold point. As can be seen from Fig. 7, the percolation situation of our model on the real network is consistent with the theoretical solution. Similar phenomena are found in real-world networks as in model networks.

6. Conclusion and future work

The main contribution of this paper is for the interdependent directed higher-order networks

research provides a theoretical framework. We constructed the fully dependence and partially dependence directed higher-order networks. We revealed the size variation of GIN, GOUT, and GSCC during percolation process, and the size of the percolation threshold. In addition, the network's percolation threshold has been calculated using the generating function and theoretical formulas, and the calculated results correspond to the Monte-Carlo simulation results.

In the experiment, we firstly constructed the fully dependence and partially dependence directed higher-order networks, and we calculated the percolation process of the GIN, the GOUT, and the GSCC in the interdependent directed higher-order networks by changing the network's hyperdegree k and hyperedge cardinality m. We found that adding higher-order edges makes the network more vulnerable. Increasing the hyperdegree distribution of heterogeneity or the hyperedge cardinality distribution of heterogeneity in interdependent directed higher-order networks will also make the network more vulnerable. Interestingly, the phase transition type changes from continuous to discontinuous with the increase of coupling strength, and partially interdependent directed higher-order networks show hybrid phase transition. Moreover, we applied the model to real-world social networks and biological neural networks for cascading failure and percolation simulation, and found that the theoretical and simulation results are consistent, and the experimental results are verified.

The results show that the model can effectively study the robustness of directed higher-order networks with different interlayer coupling intensities. For example, in bilayer interdependent biological neurons, our experimental results can verify that the amount of positive current from the synapse on one neuron A to the synapse on the other neuron B affects the function of the other neuron B. Our model captures the important impact of multi-node interactions on higher-order networks. In future work, our model can be applied to the robustness of higher-order networks with more layers or other disturbances.

Declaration of Competing Interest

The authors declare that they have no known competing financial interests or personal relationships that could have appeared to influence the work reported in this paper.

Acknowledgements

This work was supported by the National Natural Science Foundation of China under grant nos.62072412, 61902359, 61702148, and 61672468, the Opening Project of Shanghai Key Laboratory of Integrated Administration Technologies for Information Security under grant AGK2018001, the Program for Youth Innovation in Future Medicine, Chongqing Medical University, No. W0150 and the Natural Science Foundation of Chongqing, No. cstc2021jcyj-msxmX0132.

References

[1] Steven H Strogatz. Exploring complex networks. *Nature*, 410(6825):268–276, 2001.

[2] Réka Albert and Albert-László Barabási. Statistical mechanics of complex networks. *Reviews of modern physics*, 74(1):47, 2002.

[3] Stefano Boccaletti, Vito Latora, Yamir Moreno, Martin Chavez, and D-U Hwang. Complex networks: Structure and dynamics. *Physics reports*, 424(4-5):175–308, 2006.

[4] Yanyi Nie, Wenyao Li, Liming Pan, Tao Lin, and Wei Wang. Markovian approach to tackle competing pathogens in simplicial complex. *Applied Mathematics and Computation*, 417:126773, 2022.

[5] Wenyao Li, Meng Cai, Xiaoni Zhong, Yanbing Liu, Tao Lin, and Wei Wang. Coevolution of epidemic and infodemic on higher-order networks. *Chaos, Solitons & Fractals*, 168:113102, 2023.

[6] Austin R Benson, Rediet Abebe, Michael T Schaub, Ali Jadbabaie, and Jon Kleinberg. Simplicial closure and higher-order link prediction. *Proceedings of the National Academy of Sciences*, 115(48):E11221–E11230, 2018.

[7] Iacopo Iacopini, Giovanni Petri, Alain Barrat, and Vito Latora. Simplicial models of social contagion. *Nature communications*, 10(1):2485, 2019.

[8] Alain Barrat, Guilherme Ferraz de Arruda, Iacopo Iacopini, and Yamir Moreno. Social contagion on higher-order structures. In *Higher-Order Systems*, pages 329–346. Springer, 2022.

[9] Yuhang Lai, Ying Liu, Kexian Zheng, and Wei Wang. Robustness of interdependent higher-order networks. *Chaos: An Interdisciplinary Journal of Nonlinear Science*, 33(7), 2023.

[10] A Cornish-Bowden. Fundamentals of enzyme kinetics, wiley, 2012.

[11] Monica I Abrudan, Fokko Smakman, Ard Jan Grimbergen, Sanne Westhoff, Eric L Miller, Gilles P Van Wezel, and Daniel E Rozen. Socially mediated induction and suppression of antibiosis during bacterial coexistence. *Proceedings of the National Academy of Sciences*, 112(35):11054–11059, 2015.

[12] Eric D Kelsic, Jeffrey Zhao, Kalin Vetsigian, and Roy Kishony. Counteraction of antibiotic production and degradation stabilizes microbial communities. *Nature*, 521(7553):516–519, 2015.

[13] Duncan S Callaway, Mark EJ Newman, Steven H Strogatz, and Duncan J Watts. Network robustness and fragility: Percolation on random graphs. *Physical Review Letters*, 85(25):5468, 2000.

[14] Masado Ishii, Jacob Gores, and Christof Teuscher. On the sparse percolation of damage in finite non-synchronous random boolean networks. *Physica D: Nonlinear Phenomena*, 398:84–91, 2019.

[15] Hao Peng, Cheng Qian, Dandan Zhao, Ming Zhong, Jianmin Han, and Wei Wang. Targeting attack hypergraph networks. *Chaos: An Interdisciplinary Journal of Nonlinear Science*, 32(7):073121, 2022.

[16] Ming Li, Run-Ran Liu, Linyuan Lü, Mao-Bin Hu, Shuqi Xu, and Yi-Cheng Zhang. Percolation on complex networks: Theory and application. *Physics Reports*, 907:1–68, 2021.

[17] Adam Hackett, Davide Cellai, Sergio Gómez, Alexandre Arenas, and James P Gleeson. Bond percolation on multiplex networks. *Physical Review X*, 6(2):021002, 2016.

[18] Mark EJ Newman, Steven H Strogatz, and Duncan J Watts. Random graphs with arbitrary degree distributions and their applications. *Physical Review E*, 64(2):026118, 2001.

[19] SN Dorogovtsev, AV Goltsev, and JFF Mendes. k-core architecture and k-core percolation on complex networks. *Physica D: Nonlinear Phenomena*, 224(1-2):7–19, 2006.

[20] Wei Wang, Wenyao Li, Tao Lin, Tao Wu, Liming Pan, and Yanbing Liu. Generalized k-core percolation on higher-order dependent networks. *Applied Mathematics and Computation*, 420:126793, 2022.

[21] Reuven Cohen, Keren Erez, Daniel Ben-Avraham, and Shlomo Havlin. Resilience of the internet to random breakdowns. *Physical Review Letters*, 85(21):4626, 2000.

[22] Zhen Wang, Attila Szolnoki, and Matjaž Perc. If players are sparse social dilemmas are too: Importance of percolation for evolution of cooperation. *Scientific reports*, 2(1):369, 2012.

[23] Soumen Majhi, Matjaž Perc, and Dibakar Ghosh. Dynamics on higher-order networks: A review. *Journal of the Royal Society Interface*, 19(188):20220043, 2022.

[24] Unai Alvarez-Rodriguez, Federico Battiston, Guilherme Ferraz de Arruda, Yamir Moreno, Matjaž Perc, and Vito Latora. Evolutionary dynamics of higher-order interactions in social networks. *Nature Human Behaviour*, 5(5):586–595, 2021.

[25] Aanjaneya Kumar, Sandeep Chowdhary, Valerio Capraro, and Matjaž Perc. Evolution of honesty in higher-order social networks. *Physical Review E*, 104(5):054308, 2021.

[26] Luca Gallo, Riccardo Muolo, Lucia Valentina Gambuzza, Vito Latora, Mattia Frasca, and Timoteo Carletti. Synchronization induced by directed higher-order interactions. *arXiv preprint arXiv:2202.08707*, 2022.

[27] Hao Liu, Xin Chen, Long Huo, and Chunming Niu. Power network uniqueness and synchronization stability from a higher-order structure perspective. *Physica D: Nonlinear Phenomena*, 443:133557, 2023.

[28] Austin R Benson, David F Gleich, and Jure Leskovec. Higher-order organization of complex networks. *Science*, 353(6295):163–166, 2016.

[29] Hao Peng, Yifan Zhao, Dandan Zhao, Ming Zhong, Zhaolong Hu, Jianming Han, Runchao Li, and Wei Wang. Robustness of higher-order interdependent networks. *Chaos, Solitons & Fractals*, 171:113485, 2023.

[30] Ivan Bonamassa, Bnaya Gross, and Shlomo Havlin. Interdependent couplings map to thermal, higher-order interactions. *arXiv preprint arXiv:2110.08907*, 2021.

[31] Mikko Kivelä, Alex Arenas, Marc Barthelemy, James P Gleeson, Yamir Moreno, and Mason A Porter. Multilayer networks. *Journal of complex networks*, 2(3):203–271, 2014.

[32] Stefano Boccaletti, Ginestra Bianconi, Regino Criado, Charo I Del Genio, Jesús Gómez-Gardenes, Miguel Romance, Irene Sendina-Nadal, Zhen Wang, and Massimiliano Zanin. The structure and dynamics of multilayer networks. *Physics reports*, 544(1):1–122, 2014.

[33] Yu'e Wu, Guoli Yang, Yu Li, Zhipeng Zhang, Jingjing Li, and Shuhua Zhang. Evolution of cooperation in multigames on interdependent networks. *Physica D: Nonlinear Phenomena*, 447:133692, 2023.

[34] Shuhong Xue, Yunyun Yang, Biao Feng, Hailong Yu, and Li Wang. Robustness measurement of multiplex networks based on multiplex motifs. *Physica D: Nonlinear Phenomena*, page 133978, 2023.

[35] Matjaž Perc, Attila Szolnoki, and György Szabó. Restricted connections among distinguished players support cooperation. *Physical Review E*, 78(6):066101, 2008.

[36] Matjaž Perc. Does strong heterogeneity promote cooperation by group interactions? *New Journal of Physics*, 13(12):123027, 2011.

[37] Aimei Zhu. Personalised recommendation algorithm for social network based on two-dimensional correlation. *International Journal of Autonomous and Adaptive Communications Systems*, 13(2):195–209, 2020.

[38] Paolo Bartesaghi, Gian Paolo Clemente, and Rosanna Grassi. Taxonomy of cohesion coefficients for weighted and directed multilayer networks. *Chaos, Solitons & Fractals*, 166:112968, 2023.

[39] Megan Morrison and Lai-Sang Young. Chaotic heteroclinic networks as models of switching behavior in biological systems. *Chaos: An Interdisciplinary Journal of Nonlinear Science*, 32(12), 2022.

[40] Emil Saucan, RP Sreejith, RP Vivek-Ananth, Jürgen Jost, and Areejit Samal. Discrete ricci curvatures for directed networks. *Chaos, Solitons & Fractals*, 118:347–360, 2019.

[41] Yanyi Nie, Xiaoni Zhong, Tao Lin, and Wei Wang. Pathogen diversity in meta-population networks. *Chaos, Solitons & Fractals*, 166:112909, 2023.

[42] Dandan Zhao, Xianwen Ling, Xiongtao Zhang, Hao Peng, Ming Zhong, Cheng Qian, and Wei Wang. Robustness of directed higher-order networks. *Chaos: An Interdisciplinary Journal of Nonlinear Science*, 33(8), 2023.

[43] Xueming Liu, H Eugene Stanley, and Jianxi Gao. Breakdown of interdependent directed networks. *Proceedings of the National Academy of Sciences*, 113(5):1138–1143, 2016.

[44] David F Klosik, Anne Grimbs, Stefan Bornholdt, and Marc-Thorsten Hütt. The interdependent network of gene regulation and metabolism is robust where it needs to be. *Nature communications*, 8(1):534, 2017.

[45] Eben Kenah and James M Robins. Second look at the spread of epidemics on networks. *Physical Review E*, 76(3):036113, 2007.

[46] Huan Wang, Chuang Ma, Han-Shuang Chen, Ying-Cheng Lai, and Hai-Feng Zhang. Full reconstruction of simplicial complexes from binary contagion and ising data. *Nature Communications*, 13(1):1–10, 2022.

[47] Hanlin Sun and Ginestra Bianconi. Higher-order percolation processes on multiplex hypergraphs. *Physical Review E*, 104(3):034306, 2021.

[48] Joshua Faskowitz, Richard F Betzel, and Olaf Sporns. Edges in brain networks: Contributions to models of structure and function. *Network Neuroscience*, 6(1):1–28, 2022.

[49] Di Zhou, Jianxi Gao, H Eugene Stanley, and Shlomo Havlin. Percolation of partially interdependent scale-free networks. *Physical Review E*, 87(5):052812, 2013.

[50] Lav R Varshney, Beth L Chen, Eric Paniagua, David H Hall, and Dmitri B Chklovskii. Structural properties of the caenorhabditis elegans neuronal network. *PLoS computational biology*, 7(2):e1001066, 2011.

[51] Mathieu Génois and Alain Barrat. Can co-location be used as a proxy for face-to-face contacts? *EPJ Data Science*, 7(1):1–18, 2018.

[52] Xin Yuan, Yanqing Hu, H Eugene Stanley, and Shlomo Havlin. Eradicating catastrophic collapse in interdependent networks via reinforced nodes. *Proceedings of the National Academy of Sciences*, 114(13):3311–3315, 2017.